DOI 10.5012/bkcs.2010.31.02.309

Enhanced Electrochemical Properties of Surface Modified $LiMn_2O_4$ by Li-Fe Composites for Rechargeable Lithium Ion Batteries

Jin Yi Shi,[†,‡] Cheol-Woo Yi,[§,*] Lianhua Liang,[†] and Keon Kim[†,*]

[†]*Department of Chemistry, Korea University, Seoul 136-701, Korea. [*]E-mail: kkim@korea.ac.kr*
[‡]*Jilin Institute of Chemical Technology, Jilin 132022, China*
[§]*Department of Chemistry and Institute of Basic Science, Sungshin Women's University, Seoul 136-742, Korea*
[*]*E-mail: cheolwoo@sungshin.ac.kr*
Received July 11, 2009, Accepted November 7, 2009

The surface modified $LiMn_2O_4$ materials with Li-Fe composites were prepared by a sol-gel method to improve the electrochemical performance of $LiMn_2O_4$ and were characterized by X-ray diffraction (XRD), X-ray photoelectron spectroscopy (XPS), scanning electron microscopy-energy dispersive spectroscopy (SEM-EDS), and transmission electron microscopy (TEM)-EDS. XRD results indicate that all the samples (modified and pristine samples) have cubic spinel structures, and XRD, XPS, and TEM-EDS data reveal the formation of $Li(Li_xFe_xMn_{2-2x})O_4$ solid solution on the surface of particles. For the electrochemical properties, the modified material demonstrated dramatically enhanced reversibility and stability even at elevated temperature. These improvements are attributed to the formation of the solid solution, and thus-formed solid solution phase on the surface of $LiMn_2O_4$ particle reduces the dissolution of Mn ion and suppresses the Jahn-Teller effect.

Key Words: Lithium manganese oxide, Surface modification, Solid solution, Spinel, Lithium ion batteries

Introduction

$LiMn_2O_4$ has been attracted great attention as one of the most promising materials for rechargeable lithium ion batteries due to its low cost, environmental benign property, good thermal stability, high energy density, *etc*.[1-3] Even if it has been extensively studied as a potential electrode, there are still several challenges of $LiMn_2O_4$ material for lithium secondary battery such as capacity fading, manganese dissolution at elevated temperature, and poor high-rate capability. Many researchers have made tremendous efforts to improve the performance of $LiMn_2O_4$ and found that these drawbacks were mainly attributed to two factors: (i) the acid-induced dissolution of manganese ion[4,5] and (ii) Jahn-Teller effect of the high spin Mn^{3+}.[6,7] The addition of different metal ion to $LiMn_2O_4$ might be expected to suppress the Jahn-Teller effect by the increase in the oxidation state of Mn and stabilize the cubic structure. Hence, in order to solve these problems such as Mn dissolution and Jahn-Teller effect, the substitution of Mn with metal-ions, such as Co,[8,9] Ni,[8,9] Al,[1] Mg,[10] Ti[11] *etc*., has been studied and considered as an effective way to enhance the cycling stability. However, the electrochemical properties of simply doped $LiMn_2O_4$ materials have not been improved at elevated temperature under repeated charge-discharge conditions due probably to the direct contact of Mn with the electrolyte. Recently, to remedy this drawback, the surface modifications of $LiMn_2O_4$ using $Li_2O{\cdot}B_2O_3$,[12] MgO,[13] $LiCoO_2$,[14] ZnO,[15,16] CeO_2,[17] carbon,[18] or conductive polymer[19] have been studied.

In the present study, a Li-Fe composite was attempted to be a material for the surface modification of $LiMn_2O_4$ for the first time. Our modification method, as distinct from simple coating, shows the formation of $Li(Li_xFe_xMn_{2-2x})O_4$ solid solution phase on the surface of $LiMn_2O_4$ particles, and the surface modified electrodes show the dramatically improved electrochemical properties under both room and elevated temperature conditions.

Experimental

Preparation of Cathode Materials. $LiMn_2O_4$ was synthesized by a sol-gel method with citric acid. Stoichiometric amounts of $LiOH{\cdot}H_2O$ (Aldrich), $Mn(CH_3COO)_2{\cdot}4H_2O$ (Aldrich), and citric acid (Aldrich) were dissolved in the distilled water (the mole ratio of citric acid to metal ions was fixed to 1). Then ammonium hydroxide was slowly added to the solution until the pH becomes within 8.0 - 9.0, and then the solution was stirred at 80 °C to form a viscous transparent gel. The gel was subsequently heated to decompose the organic components at 450 °C for 3 hours. The obtained precursor was calcined at 850 °C for 15 hours.

The surface modification of $LiMn_2O_4$ with Li-Fe composites was performed using a sol-gel method. $LiOH{\cdot}H_2O$, $Fe(NO_3)_3{\cdot}9H_2O$, and citric acid were dissolved in the distilled water (the mole ratio of Li : Fe = 1 : 1), and then as-prepared $LiMn_2O_4$ powder was added into the solution. The compositions of Li-Fe in the modified cathode materials were 5.0 and 10 wt % named as LMO-LF5 and LMO-LF10, respectively. After the evaporation process, the solution was converted to a black gel, and it was annealed at 800 °C for 10 hours under atmospheric condition.

Physical Characterization and Electrochemical Measurement. The structure of the products was characterized by X-ray diffraction (XRD) using a Rigaku DMAX-III diffractometer equipped with a Cu target. X-ray photoelectron spectroscopy (XPS, PHI 5800 with monochromatic Al Kα, E = 1486.6 eV) was employed in examining the chemical state of Mn in pristine and modified $LiMn_2O_4$, and due to the charging effect, binding

energy scales are usually corrected using a reference peak of C 1s (284.6 eV). The morphology of the powdered product was investigated by field emission-scanning electron microscopy (FE-SEM, Hitachi S-4300, Japan) and transmission electron microscopy (TEM, JEOL JEM-2010). The dissolution behaviors of the pristine and the modified $LiMn_2O_4$ were determined by inductively coupled plasma-mass spectroscopy (ICP-MS, Elan 6100, Perkin Elemer). To find the concentrations of the dissolved Mn ions, the powdered samples were soaked in the electrolyte consisting of 1 M $LiPF_6$ in 1 : 1 mixture by volume of ethylene carbonate (EC) and dimethylcarbonate (DMC) (TECHNO Semichem Co.) at 55 °C. To determine the solubility of Mn, 0.1 g of prepared sample was transferred to 10 mL of the electrolyte in a glass vial. After a desired period, the electrolytes were filtered and analyzed.

The electrodes were prepared by mixing 10 mg of the active powder and 6.0 mg of teflonized acetylene black, and the mixture was pressed into a 1 cm^2 pellet. Then, it was dried at 120 °C for 12 hours under vacuum conditions. Lithium metal and polypropylene were used as the anode and the separator in this study, respectively. The electrolyte consists of 1.0 M $LiPF_6$ dissolved in a 1 : 1 mixture of EC and DMC. The coin-type cell (CR2032) was assembled in an argon-filled glove box. The charge-discharge tests were performed using a WBCS 3000 instrument (WonA Tech, Korea). The cyclic voltammetry (CV) and electrochemical impedance spectroscopy (EIS) were performed using IM6 electrochemical instrument (ZAHNER Elektrik, Germany).

Results and Discussion

Physical Characterization. First of all, the physical properties of pristine and surface modified $LiMn_2O_4$ samples were investigated to understand how the surface modification of $LiMn_2O_4$ with Li-Fe composites affects its properties. Fig. 1 shows the XRD results of pristine and modified $LiMn_2O_4$, and these XRD data were analyzed by Rietveld refinement. The XRD results show that pristine and modified $LiMn_2O_4$ materials have a single-phase spinel structure (cubic space group, Fd3m), and neither trace of $LiFeO_2$ nor any minor phase was observed. The lattice parameter of each sample is 8.2502(8) Å for pristine $LiMn_2O_4$, 8.2434(0) Å for LMO-LF5, and 8.2374(7) Å for LMO-LF10. It is clear that the lattice parameter slightly decreases as the amount of Li-Fe composite increases. The decrease in the lattice parameter of the modified sample is probably caused by the increase in the amount of Mn^{4+} with the smaller ionic radii than Mn^{3+}. The systematic decrease in the lattice parameter as a function of the composition of Li-Fe composite and no difference of overall XRD patterns among them are one of the evidences for the formation of a solid solution phase containing lithium, manganese and iron ions.

In order to confirm the formation of solid solution phase, XPS experiments were performed. The measured XPS spectra of Mn 2p region for pristine $LiMn_2O_4$ and LMO-LF10 are shown in Fig. 2 (a) and (b), respectively, and each spectrum was deconvoluted based on MnO_2 and Mn_2O_3 spectral lines. For the pristine sample ($LiMn_2O_4$), the XPS spectrum shows Mn $2p_{3/2}$ feature at ~ 642.4 eV which is between the binding energy

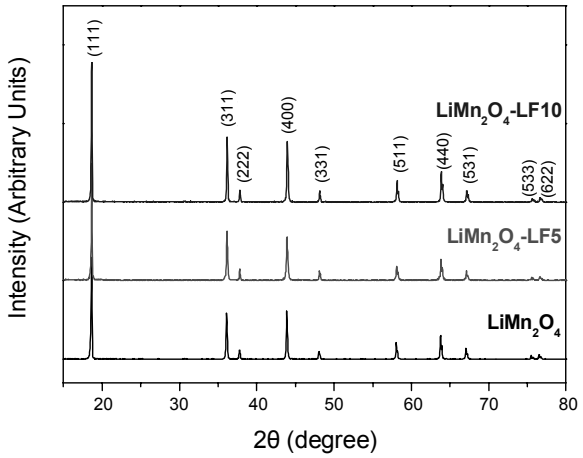

Figure 1. X-ray diffraction patterns of pristine and modified $LiMn_2O_4$ spinels.

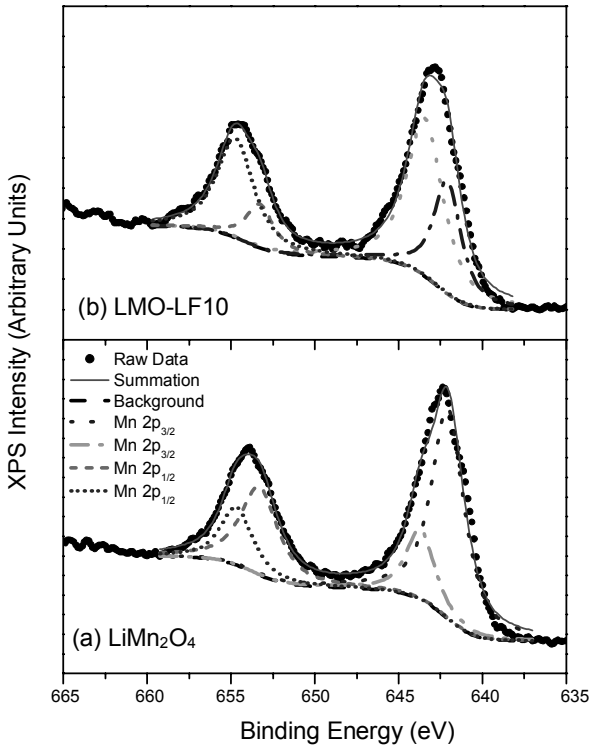

Figure 2. Mn 2p XPS spectra of (a) pristine $LiMn_2O_4$ and (b) LMO-LF10.

of MnO_2 (643.4 eV[20]) and that of Mn_2O_3 (642.0 eV[20]), and the separation of the binding energy between the Mn $2p_{3/2}$ and Mn $2p_{1/2}$ is ~ 11.6 eV which is in good agreement with published data.[21] After the modification, however, the binding energies of Mn 2p shift towards higher binding energies, and it indicates that the average oxidation number of Mn increases. Moreover, the deconvolution results show that the ratio of Mn with higher oxidation state (Mn(IV)) to Mn with lower oxidation state (Mn (III)) increases after the modification. It is in good agreement with our XRD data suggesting the decrease in their lattice parameters and the formation of solid solution after the modification. In addition, the recent study by Li *et al.*[22] reported the streng-

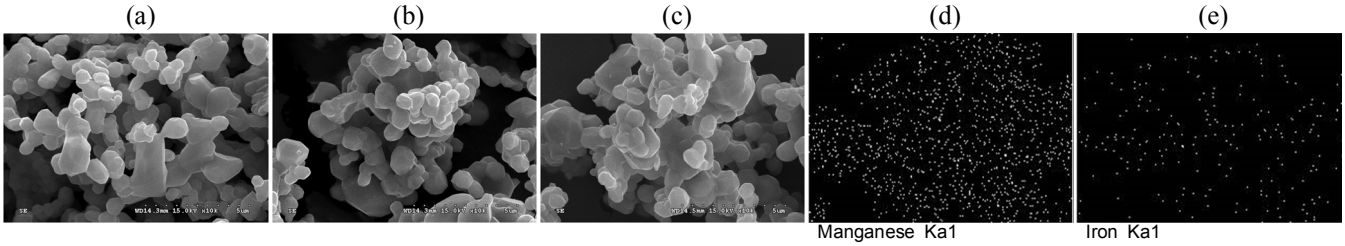

Figure 3. FE-SEM images of (a) pristine $LiMn_2O_4$, (b) LMO-LF5, and (c) LMO-LF10; EDS dot-mappings of (d) Mn and (e) Fe for modified $LiMn_2O_4$ (LMO-LF10).

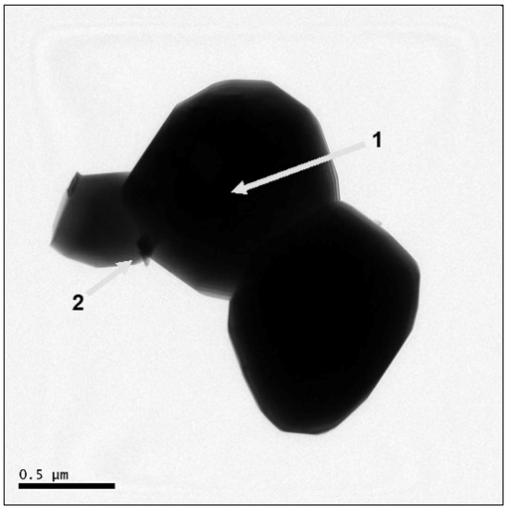

Figure 4. TEM image of sample LMO-LF10.

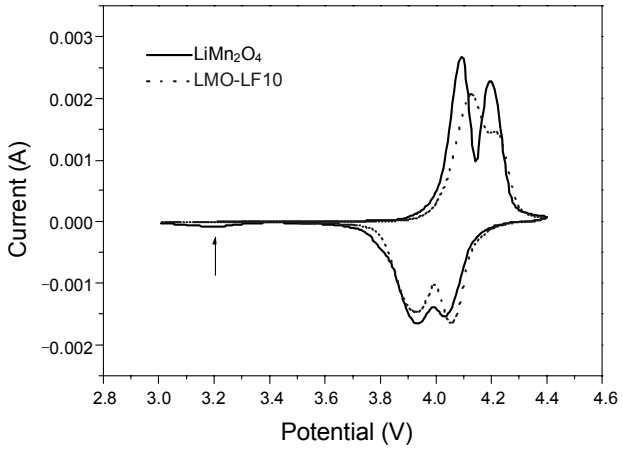

Figure 5. Cyclic voltammograms of prisitine $LiMn_2O_4$ and LMO-LF10.

thening Mn-O bond by the formation of solid solution as well as the increase in the oxidation state of Mn ion in $LiMn_2O_4$ modified by Ni using Fourier transform-infrared spectroscopy.

Morphologies of pristine and the modified $LiMn_2O_4$ samples are shown in Fig. 3 (a) - (c). The morphological difference between pristine and modified $LiMn_2O_4$ materials was not observed, and the particle size was not very different among them. Complementary EDS was performed to examine the distribution of Mn and Fe components on the surface of LMO-LF10 electrode, and the results are shown in Fig. 3 (d) and (e), respectively. The EDS images in Fig. 3 indicate that Fe and Mn components are evenly dispersed on the $LiMn_2O_4$ particles. TEM-EDS was employed in further investigating the distribution of iron ion on a LMO-LF10 single particle, and two points were selected to perform the EDS analysis as displayed in Fig. 4. Point 1 is near the center of the particle, and the concentration of iron is about 4.84 wt %. Point 2 is on the edge of the particle, and the concentration of iron is about 9.77 wt %. The iron concentration at point 2 is two times higher than that at point 1 because points 1 and 2 represent the bulk and the surface concentrations, respectively, and it suggests that the surface modified products have a coating layer on the surface of the particle which is $Li(Li_xFe_xMn_{2-2x})O_4$ solid solution. Hence, the results from XRD, XPS, and TEM-EDS strongly support that $Li(Li_xFe_xMn_{2-2x})O_4$ solid solution are formed on the surface of $LiMn_2O_4$ particles. It is readily expected that the formation of solid-solution phase causes to reduce the dissolution of Mn in the electrolyte and suppress the structural changes of the material.

Electrochemical Properties. The cyclic voltammograms (CV) of pristine $LiMn_2O_4$ and LMO-LF10 samples are presented in Fig. 5 and clearly show two couples of redox peaks at around 4.0 and 4.2 V. These CV features were considered as the characteristics of Li^+ modified spinel materials.[23,24] Tarascon *et al.*[23] reported that these two peaks originated from the Li ion extraction/reinsertion process in spinel, and the splitting between two peaks was interpreted by the cation-cation interactions. Gao *et al.*[25] suggested a simple lattice-gas model to explain the existence of the peaks in CV, and they concluded that the weakening of the peaks with increasing x in $Li_{1+x}Mn_{2-x}O_4$ is due to the presence of intercalated Li atoms pinned to the excess Li atoms substituted for Mn octahedral sites. In addition, the redox peaks of LMO-LF10 become broader than those of pristine sample due to the potential difference which depends upon the binding energy of Li ion in the different environments.[25] The presence of Fe ion in the octahedral site might slightly change the bond strength between O and Mn, and as a result, more energy is needed to extract the lithium ions from the tetrahedral sites.[24] Furthermore, a small, broad feature centered at ~ 3.2 V in CV for pristine $LiMn_2O_4$ completely disappears in LMO-LF10 as shown in Fig. 5, and this phenomenon can be explained by a Jahn-Teller transition. The peak is due to the formation of the double hexagonal-type layers in the structure, and this phase transition results in the migration of manganese ions from 16d

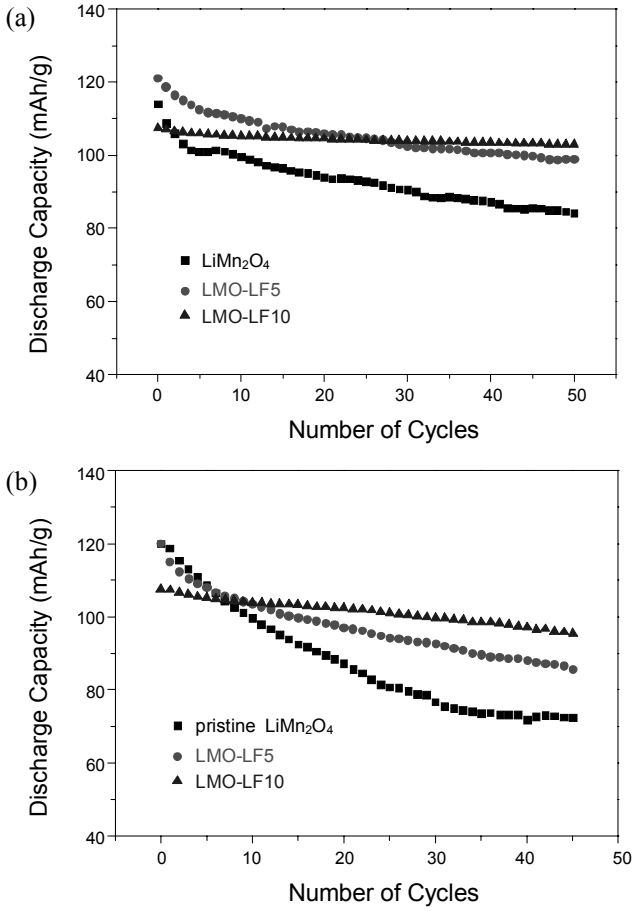

Figure 6. Cycling performance of pristine and modified $LiMn_2O_4$ in the voltage range of 3.0 - 4.4 V (a) at room temperature and (b) at 55 °C.

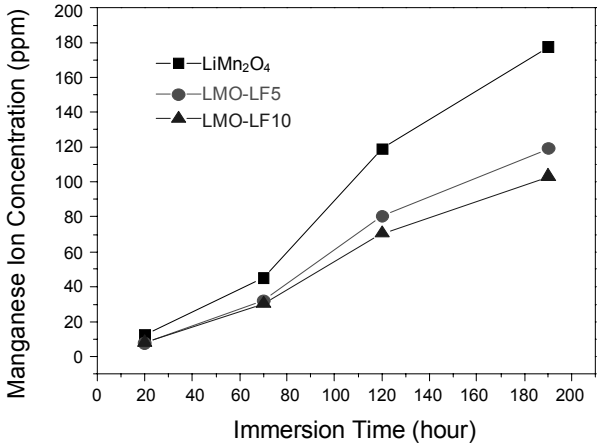

Figure 7. The relationship between the concentration of dissolved manganese cation and the immersion time for pristine and modified samples at 55 °C.

to 16c sites.[26] Therefore, the disappearance of the peak around 3.2 V on LMO-LF10 sample suggests that this surface modification can suppress the spinel-to-double hexagonal phase transition and stabilize the spinel structure during the charge and discharge process.

The cycling behaviours of pristine and modified samples were also explored to investigate their electrochemical properties. The charge-discharge cycling stability for the samples between 3.0 and 4.4 V with a constant current density of 0.5 C were examined, and the results are shown in Fig. 6. At room temperature (Fig. 6 (a)), the pristine $LiMn_2O_4$ delivered an initial discharge capacity ~ 114 mAh/g and had a value of 84.2 mAh/g after 50 charge-discharge cycles. The capacity retention ratio was 73.9 %. However, surface modified $LiMn_2O_4$ showed the enhanced cycling performance. The capacity retention ratios are 81.7 and 96.0 % for LMO-LF5 (121.1 to 98.9 mAh/g) and LMO-LF10 (107.3 to 103.0 mAh/g), respectively. Surprisingly, even at elevated temperature (55 °C), the surface modified sample showed the significantly improved cycling performance. Fig. 6 (b) shows the cyclability of pristine and modified $LiMn_2O_4$ at 55 °C, and it clearly demonstrates that the surface modification can significantly reduce the capacity fade of $LiMn_2O_4$ under elevated temperature conditions. For the pristine $LiMn_2O_4$, the discharge capacity was 119.9 mAh/g at first cycle. However, after 45 cycles, it was 72.4 mAh/g, and the retention ratio was 60.4 %. Whereas the pristine sample showed a poor performance, 71.2 and 88.7 % capacity retention ratios were measured for LMO-LF5 (120.1 to 85.5 mAh/g) and LMO-LF10 (107.6 to 95.4 mAh/g) under the same condition (55 °C), respectively. In fact, the poor performance of $LiMn_2O_4$ at elevated temperature has been one of the major issues which hinder its further commercial application, even though $LiMn_2O_4$ considered as one of the most promising cathode materials for lithium batteries. However, based on our results, surface modified $LiMn_2O_4$ materials by Li-Fe composites can overcome this problem since the surface modification by Li-Fe composite probably reduces the direct contact and suppresses the side reactions between the electrode and electrolyte. Hence, it is possible to decrease the dissolution of manganese from $LiMn_2O_4$ lattice to electrolyte and reduce the oxidation of the electrolyte on the surface of cathode at a charging period. It should be noted that this enhanced cycling behaviour of Li-Fe modified cathode may be related to the reduction of 4.2 V feature in CV as shown in Fig. 5. However, currently we do not have any direct evidence, and further study is required to understand the correlation between discharge capacities and CV results.

In order to validate the reduction of Mn dissolution by the surface modification, the concentration of Mn in the electrolyte was measured as a function of immersion time. The concentration of manganese ion in the electrolyte gradually increases as a function of immersion time as shown in Fig. 7. At 190 hours after the samples were soaked in the $LiPF_6$-containing electrolyte at 55 °C, the concentration of Mn ion in the electrolyte was ~ 180 ppm for pristine $LiMn_2O_4$. However, as we expected, the concentrations of Mn ion in the electrolyte for LMO-LF5 and LMO-LF10 were about 120 and 100 ppm, respectively, which are much lower than that of pristine sample. This result demonstrates that the surface-modified $LiMn_2O_4$ by Li-Fe composite effectively reduces the dissolution of manganese even at elevated temperature. Based on literatures,[4,5] the poor cycling performance of $LiMn_2O_4$ at elevate temperature is mainly due to severe manganese dissolution in the electrolyte in that F-containing inorganic electrolyte salt forms HF. However, the surface modification with Li-Fe composite could explicitly im-

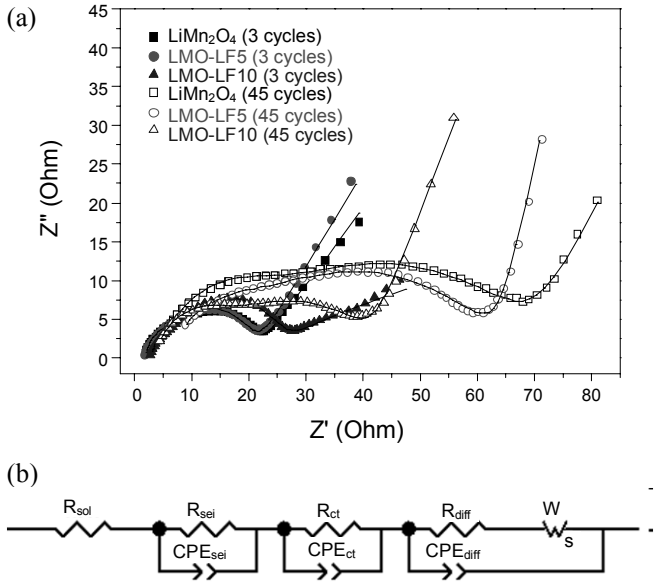

Figure 8. (a) Electrochemical impedance spectra of pristine and modified samples at different cycles. Symbols and lines represent experimental and simulated data, respectively. (b) The equivalent circuit model for impedance plot fitting.

Table 1. Impedance parameters using equivalent circuit models for pristine and modified $LiMn_2O_4$

	R_{sei} (Ω)	R_{ct} (Ω)
Pristine $LiMn_2O_4$ (3 cycles)	5.50	13.40
LMO-LF5 (3 cycles)	2.95	15.65
LMO-LF10 (3 cycles)	3.03	18.37
Pristine $LiMn_2O_4$ (45 cycles)	15.45	52.01
LMO-LF5 (45 cycles)	11.34	47.77
LMO-LF10 (45 cycles)	9.92	29.33

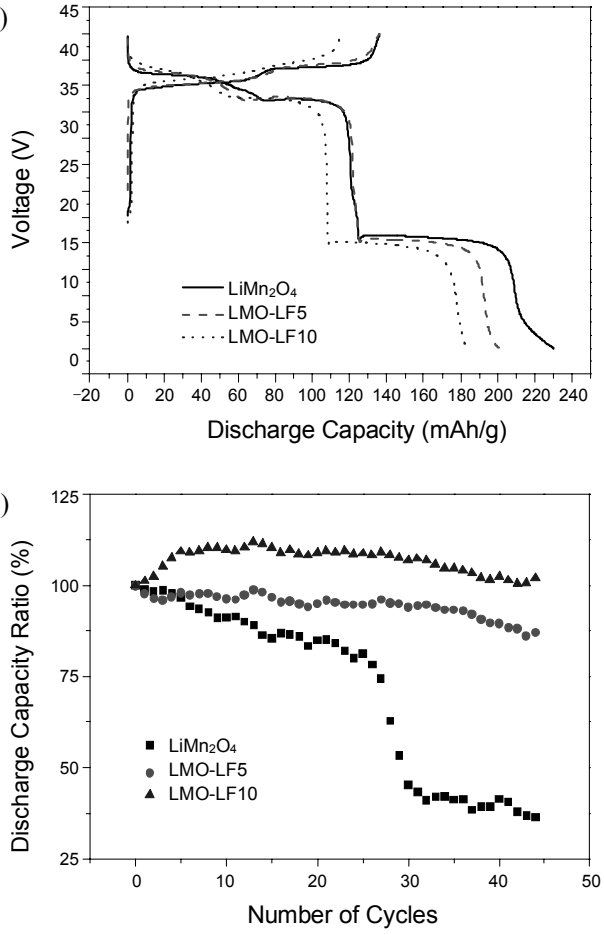

Figure 9. Electrochemical performance of pristine and modified $LiMn_2O_4$ in the voltage range of 2.0 - 4.4 V; (a) first charge-discharge curves, (b) cycling behaviours.

prove the cycling stability of the spinel $LiMn_2O_4$ cathode materials by suppressing the dissolution of manganese ions.

Electrochemical Impedance Spectroscopy (EIS). Fig. 8 (a) shows the typical impedance spectra of pristine and modified samples at the different number of charge-discharge cycles, and each curve presents two overlapped semicircles related to the multi-step of lithium ion insertion processes. The high frequency semicircle represents the resistance of the Li ion migration through the solid electrolyte interface (SEI) film (R_{sei}), the medium frequency semicircle denotes the charge transfer resistance (R_{ct}), and the low frequency inclined line is related to the diffusion of lithium ions into the bulk of the active particles (R_{diff} and the Warburg impedance (W)).[27] The parameters, R_{sei} and R_{ct} were determined by plot fitting with the equivalent circuit model shown in the Fig. 8 (b), and the results are summarized in Table 1.

Based on the results from the simulation, R_{sei} and R_{ct} are increased after 45 cycles at elevated temperature (55 °C), and the resistance changes of pristine $LiMn_2O_4$ is higher than those of modified samples. The changes of R_{sei} are 9.95, 8.39, and 6.89 Ω for pristine, LMO-LF5, and LMO-LF10 samples, respectively. The resistance of SEI film (R_{sei}) is strongly related to the thickness and species of the SEI layer,[27] and the dissolution of manganese would lead to the deposition of MnO_2, MnF_2 and LiF on the surface,[28] resulting in an increase in the resistance. However, due to the protection by the solid solution phase on the surface of the particle, the modified samples show a lower R_{sei}, which is in accordance with the dissolution test. The results of the EIS experiments also show that the pristine sample had a rapid increase in the charge transfer resistance within 45 cycles. Aurbach *et al.*[29] suggested that the charge transfer is related to the inter-particle contact which depends on physical structure of electrode materials, and this change can be attributed to manganese dissolution and Jahn-Teller effect. These two factors induce a disorder of structure and the increase in R_{ct}. As shown above, the pristine sample has higher Mn concentration in the electrolyte for dissolution test and shows a broad CV feature ~ 3.2 V related to the Jahn-Teller transition, and therefore it is evident that R_{ct} of pristine sample has higher value (after 45 cycles, R_{ct} = 52.01 Ω and ΔR_{ct} = 38.61 Ω). On the contrary, LMO-LF10 exhibits 29.33 Ω of charge transfer resistance and the increment of just 11 Ω in R_{ct} under the same cycling condition as pristine electrode. This obviously enhanced reversibility is probably originating from the modification which can stabilize its

structure during the charge-discharge processes.

Electrochemical cycling tests were performed within a wider voltage range to monitor the stability of surface modified sample since the effect of Jahn-Teller distortion becomes more significant for spinel $LiMn_2O_4$ materials in ~3.0 V region.[3] The charge-discharge profiles and cycling behaviours of pristine and modified samples between 2.0 and 4.4 V are presented in Fig. 9. Typical initial charge-discharge curves of pristine and modified samples are shown in Fig. 9 (a), and all the samples show two plateaus at ~ 3.0 and ~ 4.0 V. In $Li/Li_xMn_2O_4$ cell, when $0 < x < 1$, the cell discharges at 4.0 V with the cubic symmetry, whereas when $1 < x < 2$, the cell discharges at 3.0 V because lithium ions are intercalated into the octahedral vacancies.[3] The discharge capacities were 230 mAh/g for pristine $LiMn_2O_4$, and 200 and 183 mAh/g for LMO-LF5 and LMO-LF10, respectively. In order to investigate the reversibility as the number of charge-discharge cycle, the retention ratio of discharge capacities were measured within a voltage range of 2.0 - 4.4 V. As can be seen from Fig. 9 (b), the two modified materials exhibit an excellent cyclability as the number of cycle increases. However, the pristine sample shows a significant capacity loss (less than 50 %) after 45 cycles. Actually, the improvement of reversibility of the surface modified electrode are attributed to the iron-ions and excess lithium-ions,[30] which occupy the octahedral site in spinel structure. The existence of iron-ions and excess Li-ions in octahedral site result in a preservation of the cubic spinel phase during cycling, thus enhance the electrochemical cyclability. This result shows that the Jahn-Teller distortion of $LiMn_2O_4$ can be effectively suppressed by the surface modification with Li-Fe composite.

Conclusion

A series of surface modified $LiMn_2O_4$ by Li-Fe composites was prepared by sol-gel method with citric acid and demonstrated that the surface modified cathode materials have good electrochemical properties and cycle life. The formation of Li $(Li_xFe_xMn_{2-2x})O_4$ solid solution phase in the surface modified $LiMn_2O_4$ was confirmed by XRD, XPS, and TEM-EDS, and the solid solution phase plays an important role in the stabilization of the electrode, in that it reduces the dissolution of manganese ion from the electrode and it suppresses the Jahn-Teller effect. Moreover, they demonstrated enhanced electrochemical properties with respect to the pristine $LiMn_2O_4$ at room temperature as well as elevated temperature. Therefore, the Li-Fe composite surface modified $LiMn_2O_4$ by is one of the most promising candidate materials for practical lithium ion batteries.

Acknowledgments. This work was supported by the Research Center for Energy Conversion & Storage, Korea. This work was also supported in part by the Sungshin Women's University Research Grant of 2009.

References

1. Song, D.; Ikuta, H.; Uchida, T.; Wakihara, M. *Solid State Ionics* **1999**, *117*, 151.
2. Tarascon, J. M.; Wang, E.; Shokoohi, F. K.; McKinnon, W. R.; Colson, S. *J. Electrochem. Soc.* **1991**, *138*, 2859.
3. Thackeray, M. M.; David, W. I. F.; Bruce, P. G.; Goodenough, J. B. *Mater. Res. Bull.* **1983**, *18*, 461.
4. Aoshima, T.; Okahara, K.; Kiyohara, C.; Shizuka, K. *Mechanisms of Manganese Spinels Dissolution and Capacity Fade at High Temperature*; 10 th International Meeting on Lithium Batteries, 2000, Como, Italy.
5. Jang, D. H.; Oh, S. M. *Electrochim. Acta* **1998**, *43*, 1023.
6. Gummow, R. J.; Dekock, A.; Thackeray, M. M. *Solid State Ionics* **1994**, *69*, 59.
7. Yamada, A.; Tanaka, M.; Tanaka, K.; Sekai, K. *Jahn-Teller Instability in Spinel Li-Mn-O*; 9th International Meeting on Lithium Batteries, 1998, Edinburgh, Scotland.
8. Hosoya, M.; Ikuta, H.; Wakihara, M. *Solid State Ionics* **1998**, *111*, 153.
9. Okada, M.; Lee, Y. S.; Yoshio, M. *J. Power Sources* **2000**, *90*, 196.
10. Deng, B. H.; Nakamura, H.; Zhang, Q.; Yoshio, M.; Xia, Y. Y. *Electrochim. Acta* **2004**, *49*, 1823.
11. Krins, N.; Hatert, F.; Traina, K.; Dusoulier, L.; Molenberg, I.; Fagnard, J. F.; Vanderbemden, P.; Rulmont, A.; Cloots, R.; Vertruyen, B. *Solid State Ionics* **2006**, *177*, 1033.
12. Amatucci, G. G.; Blyr, A.; Sigala, C.; Alfonse, P.; Tarascon, J. M. *Solid State Ionics* **1997**, *104*, 13.
13. Gnanaraj, J. S.; Pol, V. G.; Gedanken, A.; Aurbach, D. *Electrochem. Commun.* **2003**, *5*, 940.
14. Park, S. C.; Kim, Y. M.; Kang, Y. M.; Kim, K. T.; Lee, P. S.; Lee, J. Y. *J. Power Sources* **2001**, *103*, 86.
15. Liu, D. Q.; Liu, X. Q.; He, Z. Z. *J. Alloy. Compd.* **2007**, *436*, 387.
16. Tu, J.; Zhao, X. B.; Xie, J.; Cao, G. S.; Zhuang, D. G.; Zhu, T. J.; Tu, J. P. *J. Alloy. Compd.* **2007**, *432*, 313.
17. Ha, H. W.; Yun, N. J.; Kim, K. *Electrochim. Acta* **2007**, *52*, 3236.
18. Liu, Z. L.; Yu, A. S.; Lee, J. Y. *J. Power Sources* **1998**, *74*, 228.
19. Arbizzani, C.; Mastragostino, M.; Rossi, M. *Electrochem. Commun.* **2002**, *4*, 545.
20. Wagner, C. D.; Naumkin, A. V.; Kraut-Vass, A.; Allison, J. W.; Powell, C. J.; John, R.; Rumble, J. *NIST X-ray Photoelectron Spectroscopy Database*.
21. Ramana, C. V.; Massot, M.; Julier, C. M. *Surf. Interface Anal.* **2005**, *37*, 412.
22. Li, X. F.; Xu, Y. L. *Appl. Surf. Sci.* **2007**, *253*, 8592.
23. Tarascon, J. M.; McKinnon, W. R.; Coowar, F.; Bowmer, T. N.; Amatucci, G.; Guyomard, D. *J. Electrochem. Soc.* **1994**, *141*, 1421.
24. Yoshio, M.; Xia, Y. Y.; Kumada, N.; Ma, S. H. *J. Power Sources* **2001**, *101*, 79.
25. Gao, Y.; Reimers, J. N.; Dahn, J. R. *Phys. Rev. B* **1996**, *54*, 3878.
26. Palacin, M. R.; Chabre, Y.; Dupont, L.; Hervieu, M.; Strobel, P.; Rousse, G.; Masquelier, C.; Anne, M.; Amatucci, G. G.; Tarascon, J. M. *J. Electrochem. Soc.* **2000**, *147*, 845.
27. Barsoukov, E.; Macdonald, J. R. *Impedance Spectroscopy: Theory, Experiment, and Applications*, 2nd ed.; Wiley-Interscience: 2005.
28. Tu, J.; Zhao, X. B.; Zhuang, D. G.; Cao, G. S.; Zhu, T. J.; Tu, J. P. *Physica B* **2006**, *382*, 129.
29. Aurbach, D.; Markovsky, B.; Levi, M. D.; Levi, E.; Schechter, A.; Moshkovich, M.; Cohen, Y. *J. Power Sources* **1999**, *81-82*, 95.
30. Xia, Y. Y.; Yoshio, M. *J. Electrochem. Soc.* **1996**, *143*, 825.